International Journal of Advanced Research and Development
ISSN: 2455-4030
Impact Factor: RJIF 5.24
www.advancedjournal.com
Volume 2; Issue 6; November 2017; Page No. 568-576

Molecular docking, Spectroscopic, NLO, NBO and antimicrobial analysis of (Z)-3-(3-bromophenyl)-1-(1H-imidazol-1-yl) prop-2-en-1-one

[1] K Kumanan, [*2] R Raj Muhamed, [3] M Raja, [4] V Sathyanarayanamoorthi, [5] M Yaseen Mowlana, [6] S Arulappan
[1, 2, 3, 6] PG & Research, Department of Physics, Jamal Mohamed College, Tiruchirappalli, Tamil Nadu, India
[3] Department of Physics, Govt Thirumagal Mills College, Gudiyattam, Vellore, Tamil Nadu, India
[4] Post Graduate and Research, Department of Physics, PSG College of Arts and Science, Coimbatore, Tamil Nadu, India
[5] PG & Research, Department of Chemistry, Jamal Mohamed College, Tiruchirappalli, Tamil Nadu, India

Abstract
The title compound of (Z)-3-(3-bromophenyl)-1-(1H-imidazol-1-yl)prop-2-en-1-one (3PIPO) have been synthesized and characterized by spectroscopic techniques. Density functional theory calculations at B3LYP/6-311++G(d) level of theory were performed for geometric parameters, natural bond orbital (NBO) and non linear optical activity analyses of synthesized compound. Stability has been analyzed using natural bond orbital of the molecule arising from hyperconjugative interactions and charge delocalization analysis. The dipole moment and first hyperpolarizabilities of the studied compounds indicate that the compound is a good candidate of nonlinear optical materials. 3PIPO compounds were screened in vitro for antimicrobial activity against three bacterial and three fungal strains and showed promising results. Molecular docking studies reveal that title compound play a vital role in bonding and results draw us to the concluded that title compound inhibit different antimicrobial proteins and that have good biological activities.

Keywords: FT-IR, FT-Raman, NLO, NBO, antimicrobial, molecular docking

1. Introduction
Heterocyclic compounds are also used in pharmacy and agriculture. Analysis of scientific papers in the last two decades revealed that there is a general trend in research for new drugs involving modification of existing biologically active matrices and molecular design of the structures of compounds. Imidazole is a highly polar one of the fivemembered nitrogen containing heterocyclic ring. It is soluble in water. The nitrogen attached with the hydrogen has a lone pair of electrons bringing the required 6 π-electrons for aromaticity. The hydrogen atom can be located on either of the two nitrogen atoms due to resonance structures of imidazole [1]. Many researchers previously proved Imidazoles and Imidazoles substituent's compounds wide range biological applications. Imidazole drugs have broadened scope in clinical medicines. Medicinal properties of imidazoles include anti-inflammatory, anticancer, anticoagulants, antifungal, antibacterial, antitubercular, antiviral, antimalarial and antidiabetic [2, 6]. Its molecular formula is C12H9BrN2O.
Based on above consideration and in continuation of our ongoing work on the development of imidazole analogues as antimicrobial agents, we report here the synthesis of (Z)-3-(3-bromophenyl)-1-(1H-imidazol-1-yl)prop-2-en-1-one (3PIPO) with anticipated antimicrobial activities, by clubbing imidazole with 3-bromophenyl groups as spacers in one frame work. The title compound has been theoretically investigated by applying density functional theory (DFT) to understand the structure activity relationship.

2. Materials and Methods
2.1. Synthesis
For the synthesis of (Z)-3-(3-bromophenyl)-1-(1H-imidazol-1-yl)prop-2-en-1-one (3PIPO) compound, the equimolar quantity of 1-acetyl imidazole (0.01 mol) and 3-Bromobenzaldehyde (0.01 mol) were dissolved in 20 ml of ethanol in a 150 mL round-bottomed flask. The reaction mixture was magnetically stirred for 3h in ice-cold condition, during stirring 10 ml of 10% sodium hydroxide solution was added dropwise. A flocculants precipitate was formed. The precipitate was filtered and washed with cold water. The solid obtained was purified by column chromatography using silica gel 60-120 mesh and n-hexane: acetone (7:3 v/v) as elevate. The reaction scheme is shown in Fig.1.

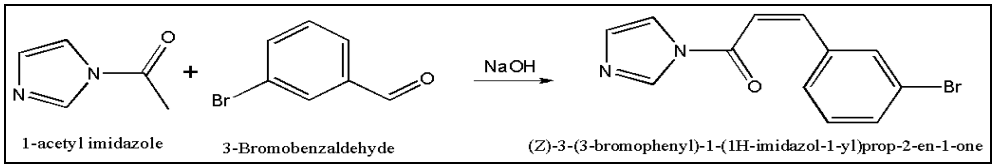

Fig 1: The scheme of the synthesis of (Z)-3-(3-bromophenyl)-1-(1H-imidazol-1-yl) prop-2-en-1-one (3PIPO)

2.2 Experimental and Computational details

The experimental FT-Raman and FT-IR spectrum of the title compound were collected from Indian Institute of Technology Madras, Chennai, India. All the quantum chemical calculations are performed by Gaussian 09W [7] software with GaussView 5.0 [8] visualization program. Additionally, the calculated vibrational frequencies were explained by means of the potential energy distribution (PED) analysis of all the fundamental vibration modes by using VEDA 4 program[9]. Molecular docking (ligand-protein) investigations have been performed by using auto Dock 4.2.6 software package.

3. Results & Discussion

3.1. Molecular Geometry

The Optimized geometrical parameters are calculated using DFT/B3LYP method with 6-311++G (d,p) higher basis set and atom numbering of title molecule is shown in Fig 2. The theoretical results are compared with related molecule such as (Z)-3-(9-Anthryl)-1-(4-chlorophenyl)-2-(4-nitro-1H-imidazol-1-yl) prop-2-en-1-one [10]. This title molecule has ten C - C bond lengths, nine C - H bond lengths, five C - N bond lengths, one (C – O, C - Br) bond length presented in title molecule and these values are listed in Table 1. The highest bond length was calculated for C9–C10 found to be 1.488 Å (experimental) and 1.493 Å (theoretical) respectively. The calculated bond length values for C-C and C-H in the benzene ring vary from 1.385-1.361 Å and 1.088-0.930 Å by B3LYP/6-311++G (d,p) basis set and well agreed with experimental values[10]. From table 1 shows the calculated and experimental results are very good agreement.

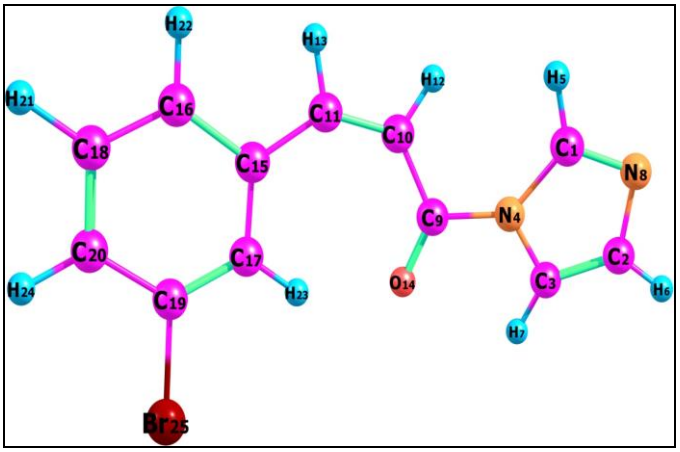

Fig 2: The theoretical optimized geometric structure with atoms numbering of 3PIPO

Table 1: Optimized geometrical parameters of (Z)-3-(3-bromophenyl)-1-(1H-imidazol-1-yl) prop-2-en-1-one (3PIPO) obtain by B3LYP/6-311++G (d,p) basis set.

Parameters	Experimental[a]	B3LYP/6-311++G (d,p)	Parameters	Experimental[a]	B3LYP/6-311++G (d,p)
Bond length(Å)			Bond angle(º)		
C1-N4	1.369	1.392	N4-C1-H5	123.9	122.8
C1-H5	0.930	1.077	N4-C1-N8	112.2	112.0
C1-N8	1.305	1.301	C1-N4-C3	106.9	105.8
C2-C3	1.357	1.361	C1-N4-C9	128.0	130.7
C2-H6	0.930	1.078	H5-C1-N8	123.9	125.2
C2-N8	1.369	1.388	C1-N8-C2	106.9	105.6
C3-N4	1.369	1.392	C3-C2-H6	127.9	128.1
C3-H7	0.930	1.075	C3-C2-N8	112.8	110.8
N4-C9	1.437	1.427	C2-C3-N4	104.2	105.8
C9-C10	1.488	1.493	C2-C3-H7	127.9	133.3
C9-O14	1.216	1.214	H6-C2-N8	123.9	121.1
C10-C11	1.355	1.355	N3-C3-H7	123.9	120.9
C10-H12	0.930	1.082	C3-N4-C9	125.0	123.4
C11-H13	0.930	1.088	N4-C9-C10	116.1	115.0
C11-C15	1.488	1.464	N4-C9-O14		118.3
C15-C16	1.415	1.410	C10-C9-O14	120.9	126.7
C15-C17	1.408	1.409	C9-C10-C11	129.3	130.4
C16-C18	1.389	1.388	C9-C10-H12	115.3	114.8
C16-H22	0.930	1.084	C11-C10-H12	115.3	114.7
C17-C19	1.389	1.388	C10-C11-H13	115.3	112.3
C17-H23	0.930	1.079	C10-C11-C15	129.3	136.7
C18-C20	1.389	1.393	H13-C11-C15	115.3	111.0
C18-H21	0.930	1.084	C11-C15-C16	117.9	115.8
C19-C20	1.389	1.393	C16-C15-C17	123.5	125.8
C19-Br25	-	1.918	C16-C15-C17	118.3	118.3
C20-H24	0.930	1.082	C15-C16-C18	121.0	121.2
			C15-C16-H22	119.3	119.3
			C15-C17-C19	119.4	119.4
			C15-C17-H23	119.8	119.8
			C18-C16-H22	119.5	119.5
			C16-C18-C20	120.4	120.2
			C16-C18-H21	120.5	120.1

			C19-C17-H23	120.7	120.7
			C17-C19-C20	122.4	122.1
			C17-C19-Br25		119.0
			C20-C18-H21	119.6	119.6
			C18-C20-C19	118.6	118.6
			C18-C20-H24	120.7	120.9
			C20-C19-Br25		118.9
			C19-C20-H24	120.5	120.5

[a]Taken from Ref [10]

3.2. Vibrational Analysis

Vibrational spectroscopy is used extensively in organic chemistry for the identification of functional groups of organic compounds, the study of molecular confirmations, kinetics, reaction etc. The (Z)-3-(3-bromophenyl)-1-(1H-imidazol-1-yl) prop-2-en-1-one (3PIPO) molecule consists of 25 atoms, which has 69 normal modes of vibration. The comparative observed and simulated FT-IR and FT-Raman spectra are shown in Fig. 3 and 4. IR intensity, Raman activity, Unscaled and Scaled frequencies are tabulated in Table 2.

3.2.1. C-H vibrations

In the heterocyclic compounds, the C-H stretching wavenumbers appear in the range 3000-3100 cm^{-1} [11]. In this present study, the C-H stretching vibrations are observed at 3137, 3114 and 3079 cm-1 by B3LYP/6-311++G (d,P) method show good agreements with experimental vibrations. The bands observed in the recorded FTIR spectrum 3107(m), 3085(m), cm-1 and 3147(w), 3080(w) cm-1 in FT-Raman. The PED corresponding to this pure mode of title molecule contributed 99, 87 and 96 % is shown in Table 2.

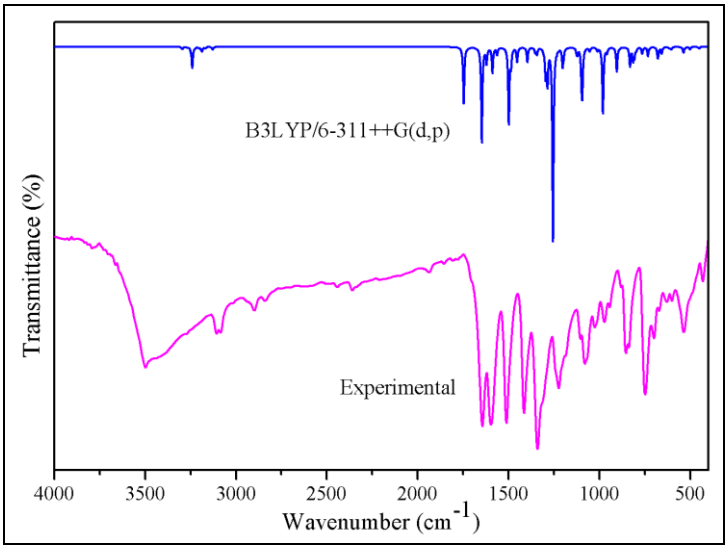

Fig 3: Experimental and theoretical FT-IR spectra of 3PIPO

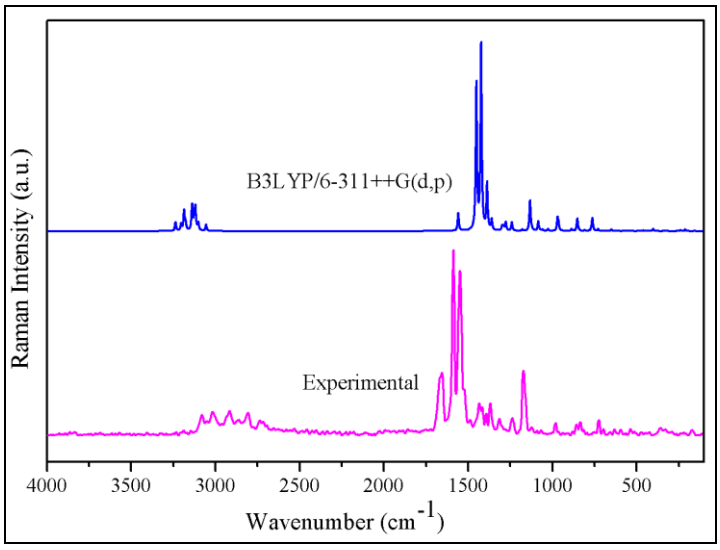

Fig 4: Experimental and theoretical FT-Raman spectra of 3PIPO

3.2.2 C-C ring vibrations

The C-C stretching vibrations are expected in the range from 1650 to 1100 cm^{-1} which are not significantly influenced by the nature of the substituents [12]. The C-C stretching vibrations of the 34FIPO compound were observed from1600 to 810 cm^{-1}. In this present study, the C-C stretching vibrations are found at 1645(vs), 1597(vs), 1515(vs), 1080(s), 1026(m), 945(m) cm^{-1} in FT-IR and 1588(vs), 1369(m), 982(w) cm^{-1} in FT-Raman respectively. The theoretical wavenumbers at 1678, 1583, 1526, 1342, 1078, 1013, 979 and 942 cm^{-1} are assigned as C-C stretching vibrations with PED contribution of 80, 50, 56, 39, 10, 12, 83 and 34% respectively.

3.2.2 C-N vibrations

The C-N stretching frequency is a very tough task since it falls in a composite region of the vibrational spectrum, i.e., mixing of several bands are possible in this region [13] assigned C-N stretching absorption in the region 1386-1266 cm-1 for the aromatic compound. The bands observed at 1224(s), 1080(s) cm-1 in FT-IR and 1393(w), 1239(m), 1066(w) in FT-Raman are assigned as C-N stretching vibrations. The theoretically scaled wavenumbers calculated at 1396, 1235, 1078 cm-1 are assigned as C-N stretching vibrations with PED contribution of 38, 67 and 37% respectively.

3.3. HOMO-LUMO analysis

The highest occupied molecular orbitals (HOMOs) and the lowest-lying unoccupied molecular orbitals (LUMOs) are named as frontier molecular orbitals (FMOs). The FMOs play an important role in the optical and electric properties, as well as in quantum chemistry. The HOMO-LUMO energies are clearly explained in molecular structural activity. So, many researchers interest to investigate structural activities in recent years. The electronic properties are precisely reported in many researchers in various organic compounds [14, 15]. The HOMO-LUMO energies and other related properties of energy gap, ionization potential (I), the electron affinity (A), the absolute electronegativity (χ), the absolute hardness (η) and softness (S) for the 3PIPO molecule have been calculated and values are given in table 3. The molecular energy transfer of 3PIPO compound is shown in Fig 5. HOMO and LUMO energy values for a molecule, electronegativity and chemical hardness can be calculated as follow:

$\chi = (I+A)/2$ (Electronegativity) (1)

$\mu = -((I+A))/2$ (Chemical potential) (2)

$\eta = (I-A)/2$ (Chemical hardness) (3)

$s=1/2\eta$ (chemical softness) (4)

$\omega=\mu 2/2\eta$ (Electrophilicity index) (5)

Where I and A are ionization potential and electron affinity; I= - EHOMO and A= - ELUMO respectively. The ground state (HOMO) energy is -6.8973 eV and the first exited state (LUMO) energy is -2.9282 eV. The ground state and first exited state energy gap of 3PIPO is found to be 3.9691 eV. Hence, the energy gap of title compound 3PIPO is low. This energy gap is elucidate the eventual charge transfer occur within the molecule.

Table 2: Calculated vibrational frequencies (cm-1) assignments of (Z)-3-(3-bromophenyl)-1-(1H-imidazol-1-yl) prop-2-en-1-one (3PIPO) based on B3LYP/6-311++G(d,p) basis set.

Mode no	Experimental wave number (cm^{-1})		Theoretical wave number(cm^{-1})		I_{IR} [c]	I_{RAMAN}[d]	Assignments (PED)[a,b]
	FTIR	FT-RAMAN	Unscaled	scaled			
69	-	-	3295	3167	1	5	γCH(95)
68	-	3147(w)	3265	3137	0	4	γCH(97)
67	-	-	3248	3122	1	11	γCH(95)
66	3107(m)	-	3240	3114	11	4	γCH(99)
65	3085(m)	3080(w)	3204	3079	0	14	γCH(87)
64	-	-	3192	3068	1	6	γCH(96)
63	-	-	3186	3062	2	11	γCH(92)
62	-	-	3170	3046	1	4	γCH(92)
61	-	3017(w)	3128	3006	1	3	γOC(96)
60	1645(vs)	-	1746	1678	29	10	γCC(80)
59	1597(vs)	1588(vs)	1647	1583	49	79	γCC(50)
58	-	-	1621	1558	8	100	γCC(55)+βHCC(16)
57	1512(vs)	-	1588	1526	13	25	γCC(56)
56	-	-	1563	1502	4	6	γCC(72)+βHCN(15)
55	-	-	1506	1447	0	3	γHCN(45)+βHCCN(20)
54	-	1435(m)	1498	1440	39	2	βHCC(38)+γHCCH(11)
53	1415(s)	-	1486	1428	8	5	βHCC(71)
52	-	1393(w)	1453	1396	7	5	γNC(38)+γHCN(13)
51	-	1369(m)	1396	1342	8	1	γCC(39)+βCC(13)
50	-	-	1353	1300	2	17	γHCC(30)+βHCN(23)
49	-	-	1344	1291	3	1	γNC(73)
48	-	-	1308	1257	1	5	γHCN(48)
47	-	-	1296	1246	14	0	βHCC(33)+γHCC(37)
46	1224(s)	1239(m)	1285	1235	18	1	γNC(67)
45	-	-	1255	1206	100	1	γHCC(15)+βHCCN(35)+γCC(10)
44	-	1172(s)	1202	1155	9	7	γHCCC(17)+βHCC(52)

43	-	-	1197	1150	3	4	γNC(33)+γCC(10)+βCNC(18)
42	-	-	1126	1082	1	1	γHCC(53)
41	1080(s)	1066(w)	1122	1078	3	0	βCC(10)+γCC(10)+γNC(37)
40	-	-	1098	1055	13	0	γHCCC(48)
39	-	-	1094	1051	21	7	γHCC(11)+βHCN(21)
38	1026(m)	-	1054	1013	2	0	γCC(12)+βHCC(12)+βHCCN(24)+βHCN(13)
37	-	982(w)	1019	979	0	1	τCC(83)
36	973(m)	-	1011	972	2	7	γHCNC(30)+βHCC(30)
35	-	-	992	953	0	0	τCC(85)
34	945(m)	940(w)	980	942	34	1	τCC(34)+βHCN(11)
33	-	905(w)	958	921	3	0	τHCCH(85)
32	881(w)	883(w)	923	887	0	0	τHCN(82)
31	-	-	909	873	0	1	βHCC(77)
30	-	-	904	869	12	0	βHCCH(-60)+βHCCH(10)
29	855(m)	857(w)	892	857	0	0	τHCCN(88)+τHCCO(10)
28	-	794(w)	832	799	10	0	τCC(77)
27	-	-	815	783	6	0	τHCCC(16)
26	-	-	807	776	5	0	τHCCN(68)
25	-	754(w)	797	766	1	0	τHCNC(65)
24	749(s)	725(w)	765	735	3	0	τHCN(10)+γHCNC(81)
23	-	-	733	704	5	0	τHCC(75)
22	-	656(w)	679	653	4	1	γCNC(13)
21	-	-	676	650	3	0	τHCNC(78)
20	629(w)	631(w)	657	632	3	0	τHCNC(89)
19	-	593(w)	616	592	1	0	τHCC(75)
18	-	564(w)	605	582	1	0	βCNC(48)
17	-	533(w)	537	516	3	0	βHCCO(58)
16	-	515(w)	528	507	0	1	τCC(71)
15	-	472(w)	503	483	1	1	γHCN(32)+βHCCC(14)
14	431(w)	448(w)	452	435	1	0	τHCCC(81)
13	-	358(w)	373	359	0	0	τCNC(68)
12	-	328(w)	332	319	2	0	βBrC(60)
11	-	-	313	301	0	1	βHCC(12)+τHCNC(21)+τHCCC(45)
10	-	292(w)	296	284	1	0	τCNC(72)
9	-	221(w)	227	218	1	0	βHCCN(52)+τHCCBr(11)
8	-	172(w)	193	185	0	0	γCNC(56)
7	-	172(w)	168	162	0	0	τCNCC(71)
6	-	-	142	137	1	0	τHCC(50)+βHCCC(14)
5	-	-	125	120	0	0	βHCCN(11)+τHCCBr(51)
4	-	-	79	76	0	0	τHCN(47)+βCC(11)
3	-	-	57	54	0	0	βBrC(10)+τHCC(27)+βCC(13)
2	-	-	24	23	0	0	τCNCC(76)
1	-	-	13	13	0	0	τ HCCN (73)

[a]γ-stretching, β- bending, τ-torsion, vs-very strong, s- strong, m-medium, w-weak, vw-very weak.
[b]scaling factor : 0.961 for B3LYP/6-311+G(d,p)
[c]Relative absorption intensities normalized with highest peak absorption equal to 100.
[d]Relative Raman intensities normalized to 100.

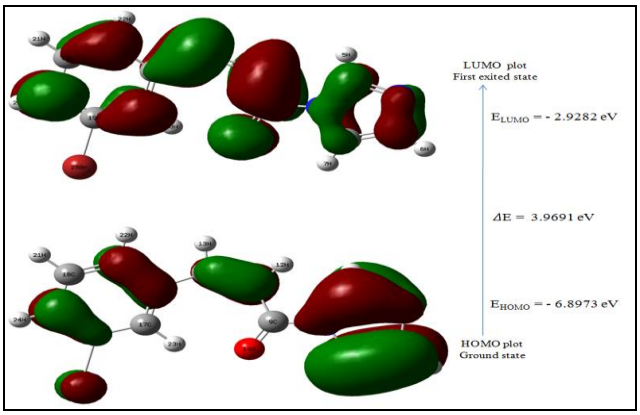

Fig 5: Highest occupied and lowest unoccupied molecular orbital of 3PIPO obtain with B3LYP/6-311++G (d,p) method

Table 3: Calculated energy values of title compound by B3LYP/6-311++G (d,p) method.

Basis set	B3LYP/6-311++G(d,p)
E_{Homo}(eV)	-6.8973
E_{Lumo}(eV)	-2.9282
Ionization potential	6.8973
Electron affinity	2.9282
Energy gap(eV)	3.9691
Electronegativity	4.9128
Chemical potential	-4.9128
Chemical hardness	1.9846
Chemical softness	0.2519
Electrophilicity index	6.0808

3.3. NLO Activity

The non linear optical properties are calculated theoretically using same theoretical methodology. M. Raja *et al* [16] reported first order hyperpolarizability, total dipole moments and polarizability of organic compound. P. Rajesh *et al* [15] reported NLO activity compounds used to many communications systems. The title compound calculated NLO result compare to Urea compounds. Urea is one of the standard NLO activity molecules. It is used to comparative purpose only. The calculated dipole moment and hyperpolarizability values obtained from B3LYP/6-311++G (d,p) methods are listed in Table 4. The first order hyperpolarizability of 3PIPO with B3LYP/6-311++G (d,p) basis set is 12.5860 x 10^{-30} twenty times greater than the value of urea (βo = 0.6230 x 10^{-30} esu).

Table 4: The values of calculated dipole moment μ (D), polarizability (α_0), first order hyperpolarizability (βtot) components of 3PIPO

Parameters	B3LYP/6-311++G (d,p)	Parameters	B3LYP/6-311++G (d,p)
μ_x	-2.3735	β_{xxx}	-1158.6803
μ_y	0.4154	β_{xxy}	-133.3448
μ_z	0.2752	β_{xyy}	-31.9993
μ(D)	2.4252	β_{yyy}	101.6175
α_{xx}	303.6340	β_{zxx}	-543.9556
α_{xy}	24.4427	β_{xyz}	-46.957
α_{yy}	126.5590	β_{zyy}	82.0438
α_{xz}	54.0248	β_{xzz}	-248.146
α_{yz}	31.9933	β_{yzz}	44.9558
α_{zz}	207.5966	β_{zzz}	234.1959
α_0 (e.s.u)	$3.1507x10^{-23}$	βtot (e.s.u)	$12.5860X10^{-30}$
Δα(e.s.u)	$8.1193x10^{-23}$		

3.4. NBO analysis

NBO analysis is clearly identified molecular nature of donor-acceptor interactions. The many researchers precisely calculated for donor (i)-acceptor (j) integrations and the stabilization energy by using the second-order micro-disturbance theory [17]. A useful aspect of the NBO method is that it gives information about interactions in both filled and virtual orbital spaces that could enhance the analysis of intra- and intermolecular interactions. The higher the E (2) value, the molecular interaction between electron donors and electron acceptors is more intensive and the greater the extent of conjugation of the entire system. Some important second order perturbation energies and molecular orbital interactions investigated from the NBO calculation are listed in Table 5, which shows the very important interactions between Lewis and non-Lewis orbital with Oxygen and nitrogen lone pairs. The very significant interaction between them was the electron donation of LP(1) N_4, LP(2) N_8, LP(2) O_{14} and LP (3) Br_{25} to the neighbouring antibonding acceptor $\pi^*(C_1\text{-}N_8)$, $\pi^*(C_2\text{-}C_3)$, $\sigma^*(C_1\text{-}N_4)$, $\sigma^*(N_4\text{-}C_9)$, $\pi^*(C_9\text{-}C_{10})$ and $\pi^*(C_{19}\text{-}C_{20})$ of the 3PIPO energy by 17.190, 12.440, 9.060, 24.500, 9.870 and 10.150 kJ/mol.

Table 5: Second order perturbation theory analysis of Fock matrix in NBO basis for (Z)-3-(3-bromophenyl)-1-(1H-imidazol-1-yl) prop-2-en-1-one

Donor(i)	Type	ED/e	Acceptor(i)	Type	ED/e	[a]E(2) (KJ mol^{-1})	[b]E(J)-E(i) (a.u.)	[c]F(I,j) (a.u.)
C_1-N_4	σ	1.9660	C_3-H_7	σ*	0.0113	2.920	1.170	0.052
			C_9-O_{14}	π*	0.3155	3.940	0.690	0.050
C_1-H_5	σ	1.9836	C_1-N_8	σ*	0.0072	0.860	1.150	0.028
			C_2-N_8	σ*	0.0167	3.870	0.950	0.054
			C_3-N_4	σ*	0.0221	1.680	0.910	0.035
C_1-N_8	σ	1.9887	C_2-H_6	σ*	0.0126	2.260	1.310	0.049
C_1-N_8	π	1.9272	C_2-C_3	π*	0.1669	11.540	0.350	0.058
C_2-C_3	π	1.9026	C_1-N_8	π*	0.2213	9.400	0.280	0.047
C_2-H_6	σ	1.9857	C_3-N_4	σ*	0.0221	2.850	0.880	0.045
C_2-N_8	σ	1.9727	C_1-N_4	σ*	0.0533	2.260	0.990	0.043
			C_1-H_5	σ*	0.0188	5.060	1.110	0.067
			C_3-H_7	σ*	0.0113	3.470	1.140	0.056
C_3-N_4	σ	1.9758	C_1-H_5	σ*	0.0188	2.450	1.140	0.047
			C_2-H_6	σ*	0.0126	2.990	1.180	0.053

N_4-C_9	σ	1.9714	C_{10}-C_{11}	σ*	0.0175	2.980	1.070	0.050
C_9-O_{14}	π	1.9618	C_{10}-C_{11}	π*	0.2089	5.800	0.320	0.040
C_{10}-C_{11}	σ	1.9822	N_4-C_9	σ*	0.0940	3.950	0.940	0.056
C_{10}-C_{11}	π	1.7180	C_9-O_{14}	π*	0.3155	41.790	0.230	0.088
			C_{15}-C_{17}	π*	0.3880	12.900	0.260	0.053
C_{10}-H_{12}	σ	1.9805	C_9-O_{14}	σ*	0.0278	5.650	1.010	0.068
			C_{11}-C_{15}	σ*	0.0232	3.940	1.090	0.059
C_{11}-H_{13}	σ	1.9698	C_9-C_{10}	σ*	0.0386	3.210	1.030	0.051
			C_{15}-C_{17}	σ*	0.0339	7.030	1.310	0.086
C_{11}-C_{15}	σ	1.9790	C_{15}-C_{16}	σ*	0.0264	2.630	1.740	0.060
			C_{15}-C_{17}	σ*	0.0339	3.510	1.540	0.066
C_{15}-C_{16}	σ	1.9682	C_{10}-C_{11}	σ*	0.0175	5.130	1.060	0.066
			C_{11}-C_{15}	σ*	0.0232	5.080	1.260	0.072
			C_{15}-C_{17}	σ*	0.0339	3.390	1.520	0.064
			C_{16}-C_{18}	σ*	0.0148	3.110	1.260	0.056
C_{15}-C_{17}	σ	1.9626	C_{11}-C_{15}	σ*	0.0232	3.390	1.250	0.058
			C_{15}-C_{16}	σ*	0.0264	2.070	1.710	0.053
			C_{17}-C_{19}	σ*	0.0255	3.650	1.260	0.061
			C_{19}-Br_{25}	σ*	0.0341	5.070	0.810	0.057
C_{15}-C_{17}	π	1.5556	C_{10}-C_{11}	π*	0.2089	30.540	0.230	0.080
			C_{16}-C_{18}	π*	0.2909	20.810	0.270	0.070
			C_{19}-C_{20}	π*	0.3720	17.690	0.260	0.062
C_{16}-C_{18}	σ	1.9768	C_{11}-C_{15}	σ*	0.0232	4.280	1.260	0.066
			C_{15}-C_{16}	σ*	0.0264	2.370	1.720	0.057
			C_{18}-C_{20}	σ*	0.0172	2.390	1.270	0.049
			C_{20}-H_{24}	σ*	0.0138	2.250	1.160	0.046
C_{16}-C_{18}	π	1.6622	C_{15}-C_{17}	π*	0.3880	18.300	0.290	0.066
			C_{19}-C_{20}	π*	0.3720	23.290	0.270	0.072
C_{16}-H_{22}	σ	1.9803	C_{15}-C_{17}	σ*	0.0339	3.560	1.350	0.062
			C_{18}-C_{20}	σ*	0.0172	3.380	1.100	0.054
C_{17}-C_{19}	σ	1.9805	C_{15}-C_{16}	σ*	0.0264	8.030	1.740	0.106
			C_{15}-C_{17}	σ*	0.0339	13.260	1.540	0.128
C_{17}-H_{23}	σ	1.9763	C_{19}-C_{20}	σ*	0.0271	4.280	1.070	0.060
C_{18}-C_{20}	σ	1.9717	C_{19}-C_{20}	σ*	0.0271	3.680	1.270	0.061
			C_{19}-Br_{25}	σ*	0.0341	5.230	0.820	0.059
C_{19}-C_{20}	π	1.6392	C_{15}-C_{17}	π*	0.3880	22.410	0.300	0.074
			C_{16}-C_{18}	π*	0.2909	16.400	0.290	0.063
C_{19}-Br_{25}	σ	1.9850	C_{15}-C_{17}	σ*	0.0339	12.310	1.460	0.120
C_{20}-H_{24}	σ	1.9788	C_{16}-C_{18}	σ*	0.0148	3.520	1.080	0.055
			C_{17}-C_{19}	σ*	0.0255	4.140	1.090	0.060
N_4	LP(1)	1.7149	C_1-N_8	π*	0.2213	17.190	0.360	0.071
			C_2-C_3	π*	0.1669	12.440	0.390	0.064
			C_9-O_{14}	σ*	0.0278	7.660	0.810	0.075
			C_9-O_{14}	π*	0.3155	4.850	0.330	0.036
N_8	LP(1)	1.9220	C_1-N_4	σ*	0.0533	9.060	0.690	0.071
			C_2-C_3	σ*	0.0139	3.030	1.010	0.050
O_{14}	LP(1)	1.9767	C_9-C_{10}	σ*	0.0386	3.400	1.240	0.058
O_{14}	LP(2)	1.8833	N_4-C_9	σ*	0.0940	24.500	0.580	0.107
			C_9-C_{10}	σ*	0.0386	9.870	0.790	0.080
Br_{25}	LP(2)	1.9744	C_{17}-C_{19}	σ*	0.0255	3.370	0.840	0.048
			C_{19}-C_{20}	σ*	0.0271	3.540	0.840	0.049
Br_{25}	LP(3)	1.9312	C_{19}-C_{20}	π*	0.3720	10.150	0.290	0.053

[a]E(2) means energy of hyper conjugative interaction (stabilization energy)
[b]Energy difference between donor and acceptor i and j NBO orbitals.
[c]F(i,j) is the Fock matrix element between i and j NBO orbitals

3.5. Antimicrobial studies

Antimicrobial (antibacterial and antifungal) activity of DMSO extracts with different concentration (25, 50, 75 and 100 µl) inhibition Zone (mm) in agar well diffusion method is tabulated in Tables 6. To further examine the in vitro activity of (Z)-3-(3-bromophenyl)-1-(1H-imidazol-1-yl)prop-2-en-1-one (3PIPO) compound and results was compared to standard drug of Erythromycin. Title compound is more active *Moraxella*, *Enterobacter*, Pseudomonas aeruginosa, *Candida albicans*, A.niger and *Trichophyton* compared than standard drug. Together, these results indicate that 3PIPO shows broad-spectrum antimicrobial activity against. The activities of 3PIPO against bacterial and fungal pathogens are shown in Fig.6.

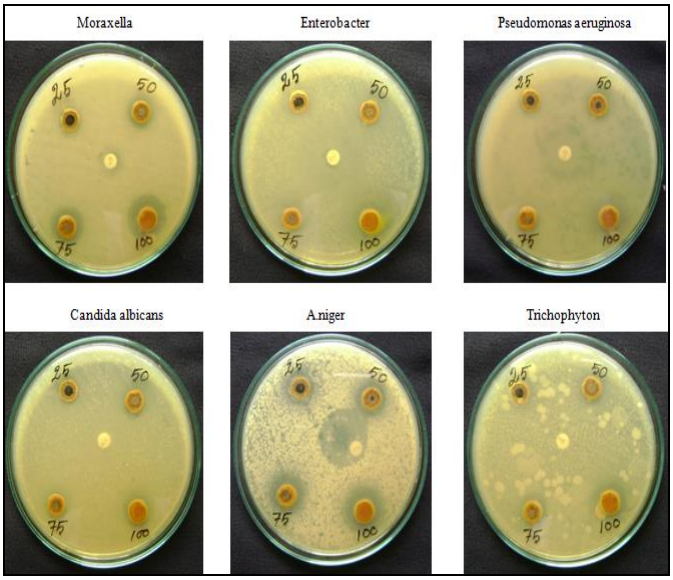

Fig 6: Antibacterial activity and antifungal activity of title molecule

3.6. Molecular docking

Molecular docking is a key tool in structural molecular biology and computer-assisted drug design. Auto Dock is a collection of automated docking tools arrange to predict how miniature scale molecules, such as substrates or drug candidate, bind to a receptor of known three dimensional structures.

Table 6: Antimicrobial activity of 3PIPO

Organism	DMSO Extract added and Zone of inhibition (mm/ml)				
	Control	25 µl	50 µl	75 µl	100 µl
Moraxella	10	12	14	16	20
Enterobacter	20	15	20	25	30
P. aeruginosa	20	11	14	16	20
Candida albicans	10	12	15	18	22
A. niger	24	13	15	18	21
Trichophyton	09	10	13	15	19

The aim to investigate the binding mode, a molecular modeling study was performed and 3PIPO was selected to be docked into the active site of three receptors 3F03, 4UM7 and 4HOE [18] of antimicrobial proteins which was downloaded from RCSB protein data bank [19]. Docked conformation which had the lowest binding energy was chosen to investigate the mode of binding. The molecular docking binding energies (kcal/mol) and inhibition constants (µm) were also obtained and listed in Table 7. Among them, 4HOE exhibited the lowest free energy at -7.16 kcal/mol and most docked inhibitors interacted with the ligand within the 4HOE binding site. They exhibited up to two hydrogen bonds involving GLY 114 and THR 58 with RMSD being 27.78 Å. The docking simulation shows the best binding mode of the 3PIPO into 3EQA. The 3PIPO ligand interacts with different receptors are shown in Figs.7-9.

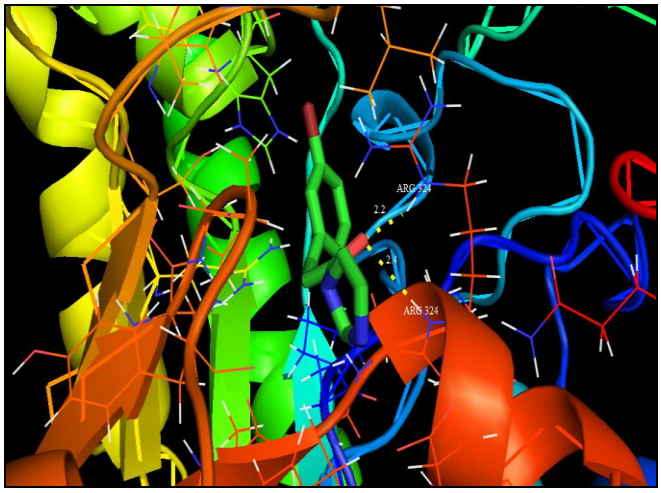

Fig 7: Docking and Hydrogen bond interactions 3PIPO with chain A of 3F03 protein structure

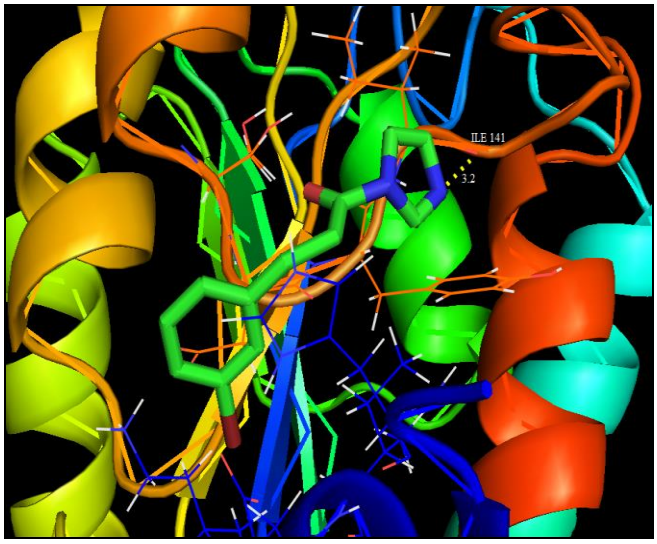

Fig 8: Docking and Hydrogen bond interactions 3PIPO with chain A of 4UM7 protein structure

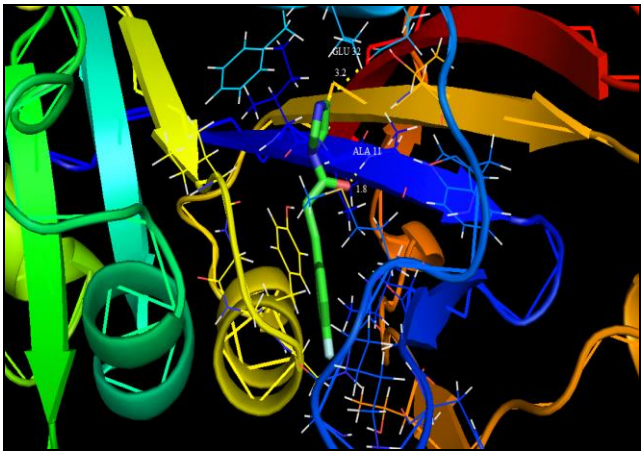

Fig 9: Docking and Hydrogen bond interactions 3PIPO with chain A of 4HOE protein structure

Table 7: Hydrogen bonding and molecular docking with antimicrobial protein targets

Protein (PDB ID)	Bonded residues	No. of hydrogen bond	Bond distance (Å)	Estimated Inhibition Constant (µm)	Binding energy (kcal/mol)	Reference RMSD (Å)
3F03	ARG 324	2	3.2	51.61	-5.85	39.01
	ARG 324		2.4			
4UM7	ILE 141	1	3.2	161.72	-5.17	21.68
4HOE	GLY 114	2	1.9	5.62	-7.16	27.78
	THR 58		2.6			

4. Conclusions

In this present work, we have reported on complete structural activity, vibrational and electronic properties of synthesized (Z)-3-(3-bromophenyl)-1-(1H-imidazol-1-yl)prop-2-en-1-one compound using spectroscopic and computational technique. The vibrational frequencies of the fundamental modes of the compound have been accurately assigned and investigated. Theoretical results were compared with the experimental vibrations. The calculated first hyperpolarizability of the title compound is 12.5860 x 10-30 esu which is comparable with the reported values of similar derivatives and which is twenty times that of the standard NLO material urea. Stability of the molecule arising from hyperconjugative interaction and charge delocalization has been analyzed using NBO analysis. The synthesized compound was tested against three different bacterial and three different fungal strains are exhibited moderate to good activity.. The molecular docking output shows that the lowest binding energy for 3PIPO is -7.16 kcal/mol and most docked inhibitors interacted with the ligand within the 4HOE binding site.

5. References

1. Verma A, Joshi S, Singh D. Imidazole: Having versatile biological activities. J Chem, 2013, 1-12.
2. Congiu C, Cocco MT, Onnis V. Design, synthesis and in vitro antitumor activity of new 1, 4-diarylimidazole-2-ones and their 2-thione analogues. Bioorg Med Chem Lett, 2008; 18:989-993.
3. Siddiqui IR, Singh PK, Srivastava V, Singh J. Facile synthesis of acyclic analogues of carbocyclic nucleoside as potential anti-HIV pro-drug. Indian Journal of Chemistry, 2010; 49B:512-520.
4. Lin YI, Peterson PJ, Yang Y, Weiss WJ, Shales DM. 5,5,6-Fused tricycles bearing imidazole and pyrazole 6-methylidene penems as broad-spectrum inhibitors of ß-lactamases. Bioorg Med Chem Lett, 2008; 16:1890-1902.
5. Nakamura T, Kakinuma H, Umemiya H, Amada H, Miyata N. Imidazole derivatives as new potent and selective 20-HETE synthase inhibitors. Bioorg Med Chem Lett, 2004; 14:333-336.
6. Roman G, Riley JG, Vlahakis JZ, Kinobe RT, Brien JF. Heme oxygenase inhibition by 2-oxy-substituted 1-(1H-imidazol-1-yl)-4- phenylbutanes: effect of halogen substitution in the phenyl ring. Bioorg Med Chem, 2007; 15:3225-3234.
7. Frisch MJ, Trucks GW, Schlegel HB, Scuseria GE, Robb MA. Gaussian 09, Revision E.01, Gaussian, Inc., Wallingford CT, 2009.
8. GaussView, Version 5, Roy Dennington, Todd Keith, and John Millam, *Semichem Inc.*, Shawnee Mission, KS, 2009.
9. Jamroz MH, Vibrational Energy Distribution Analysis VEDA 4, Warsaw, 2004.
10. Wang GZ, Lu YH, Zhou CH, Zhang YY, (Z)-3-(9-Anthryl)-1-(4-chlorophenyl)-2-(4-nitro-1H-imidazol-1-yl)prop-2-en-1-one, Acta Cryst. E65, 2009, 1113.
11. Swarnalatha N, Gunasekaran Muthu S, Nagarajan M. Molecular structure analysis and spectroscopic characterization of 9-methoxy-2H-furo[3,2-g]chromen-2-one with experimental FT-IR and FT-Raman techniques and quantum chemical calculations, spectrochim. Acta part A, 2015; 137:721-729.
12. Sundaraganesan N, Illakiamani S, Meganathan C, Joshua BD. Vibrational spectroscopy investigation using ab initio and density functional theory analysis on the structure of 3-aminobenzotrifluoride, Spectrochim. Acta A, 2007; 67:214-224.
13. Silverstein RM, Basseler GC, Morill C. Spectrometric Identification of Organic Compounds, Wiley, New York, 1981.
14. Vanasundari K, Balachandran V, Kavimani M, Narayana B. Molecular docking, vibrational, structural, electronic and optical studies of {4 – (2, 6) dichlorophenyl amino 2-methylidene 4–oxobutanoic acid and 4- (2, 5)}dichlorophenyl amino 2-methylidene 4 – oxobutanoic acid – A comparative study, Journal of Molecular Structure, 2018; 1155:21-38.
15. Rajesh P, Gunasekaran S, Gnanasambandan T, Seshadri S. Experimental, quantum chemical and NBO/NLMO investigations of pantoprazole, Spectrochimica Acta Part A: Molecular and Biomolecular Spectroscopy, 2015; 136:247-255.
16. Raja M, Raj Muhamed R, Muthu S, Suresh M, Synthesis. Spectroscopic FT-IR, FT-Raman, NMR, UV-Visible, NLO, NBO, HOMO-LUMO, Fukui function and molecular docking study of (E)-1-(5-bromo-2-hydroxybenzylidene) semicarbazide, Journal of Molecular Structure, 2017; 1141:284-298.
17. Srinivasaraghavan R, Thamaraikannan S, Seshadri S, gnanasambandan T, Spectrochim. Molecular conformational stability and Spectroscopic analysis of Parared with experimental techniques and quantum chemical calculations, Acta A, 2015; 137:1194-1205.
18. Ravi Kumar A, Sathaiah G, Chandra Shekhar A, Raju K, Shanthan Rao P, Narsaiah B *et al.* Synthesis of 6-Fluoro-7-cyclic Amino-substituted Dicarboxylic Acid Quinolones and their Antibacterial Activity, J. Hetercycl Chem, 2014; 51:114-122.
19. Joselin Beaula T, Hubert Joe I, Rastogi VK, Bena Jothy V, Spectral investigations. DFT computations and molecular dockingstudies of the antimicrobial 5-nitroisatin dimer, Che. Phy. Letters, 2015; 624:93-101.